A NOVEL THRESHOLD DETECTION METHOD FOR FMCW RADAR

Yuankai Wang[1], Zelong Xiao[1*], Jianzhong Xu[1]

[1]School of Electronic and Optical Engineering, Nanjing University of Science and Technology, Nanjing, China

** zelongxiao@mail.njust.edu.cn*

Keywords: FMCW, detection probability, false alarm, sampling loss, CZT.

Abstract

In frequency-modulated continuous-wave (FMCW) radar, fast Fourier transform (FFT) is applied as a spectrum analyser for beat signal and threshold detection is usually performed on the spectral magnitudes. The picket fence effect of FFT can cause a magnitude loss of the spectral line corresponding to a target, and therefore degrades the detection performance. To analyze this phenomenon in detail, this paper examines the statistical properties of the discrete spectrums of Gaussian noise and beat signal embedded in Gaussian noise, and derives mathematical expressions of false alarm probability and detection probability for FMCW radar. To alleviate the loss caused by the picket fence effect, this paper presents a novel threshold detection method that combines FFT and chirp z-transform (CZT). Simulation results indicate that the proposed method can improve detection probability while reducing false alarm rate, with high operation speed when the number of targets is low.

1 Introduction

Frequency-modulated continuous-wave (FMCW) radars have been widely used in various applications such as automotive adaptive cruise control (ACC), missile guidance and microwave level measurement. Compared with pulse radar, FMCW radar has relatively low transmitting peak power and can be implemented by simple hardware and architecture [1].

In FMCW radar, the range of a target is proportional to the frequency of the beat signal obtained by mixing the received signal and transmitted signal. Fast Fourier transform (FFT) is usually applied as a spectrum analyser for the beat signal. The output signal from the spectrum analyser, which is actually the magnitude spectrum, can be best referred as the video signal and will be further processed like in pulse radar [2], i.e. threshold detection is performed.

To study the detection performance of FMCW radar, including false alarm probability and detection probability, the statistical properties of the beat signal spectrum should be derived first. However, there is a lack of detailed analysis about that. In this study, we derived probability density function (PDF) of the discrete spectral magnitudes of Gaussian noise and beat signal embedded in Gaussian noise. As a result, mathematical expressions for false alarm probability and detection probability of FMCW radar were obtained. From these mathematical expressions, we can know how the picket fence effect of FFT causes a loss of detection probability. The loss has been regarded as a "straddle loss" [2]. However, this kind of loss is more like sampling loss according to the description of straddle loss [3] and the definition of sampling loss [4].

In order to reduce the loss caused by the picket fence effect, a detector using frequency shifts has been proposed [5]. However, the detector still does not take full advantage of the frequency information and has a slightly higher average false alarm rate than a regular detector. In fact, zero-padding FFT with large number of points can alleviate the picket fence effect and is more useful to deal with this kind of loss. Nevertheless, the computational cost of zero-padding FFT is very high. To improve the operation efficiency, we propose a new threshold detection method, which utilizes FFT and a low "threshold" to filter out the useless spectral regions, and applies CZT and a high threshold for the final detection.

2 Principles of FMCW Radar

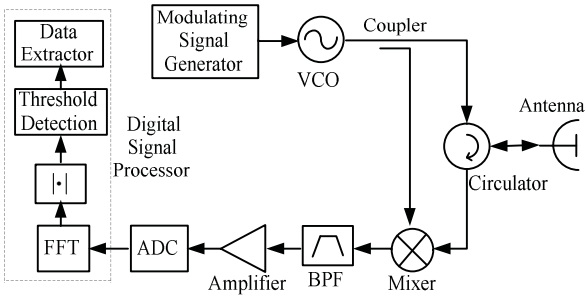

Figure 1. Configuration of a FMCW radar system.

A simplified configuration of a FMCW radar system is illustrated in Figure 1. Linear frequency modulation signal is generated by the VCO, which is controlled by the output voltage of a modulating signal generator, and is radiated by the antenna. The echo signal reflected by a target is received by the antenna and mixed with a portion of transmitted signal to obtain the beat signal. A band-pass filter is utilized to suppress the low frequency components induced by parasitic amplitude modulation, and to filter out the high frequency components that can cause spectrum aliasing after sampling in time-domain. The filtered beat signal is amplified and then converted to digital signal by an ADC. Digital signal processing based on FFT is

carried out and threshold detection is performed on the spectral magnitudes of the beat signal. At the output of the data extractor, the range information of detected targets is extracted.

The beat signal in one modulation period can be expressed as [1]

$$s(t) = A\cos\left[2\pi\Delta F_{\mathrm{m}}\tau\frac{t}{T} + 2\pi f_0\tau\right], \quad (1)$$

where A is the amplitude, T is the modulation period , f_0 is the starting frequency, ΔF_{m} is the tuning bandwidth, τ is the round-trip time delay. The relationship between the beat frequency f_{b} and the range R of a target is $f_b = \Delta F_m\tau / T = 2R\Delta F_m / cT$.

3 Detection Performance Analysis for FMCW Radar

In pulse radar, threshold detection is performed on the video signal. In order to obtain the mathematical expression for false alarm probability, the PDF of the output signal of envelope detector with Gaussian noise at its input was derived. In the same manner, mathematical expression for detection probability was derived, assuming that the input signal of the envelop detector is a sine wave along with Gaussian noise [3]. Similar analysis method can be applied in FMCW radar. Because threshold detection is performed on the spectral magnitudes of the beat signal, the PDF of the spectral magnitudes of Gaussian noise and beat signal embedded in Gaussian noise should be derived.

3.1 False Alarm Probability

The continuous-time Fourier transform (CTFT) of Gaussian noise does not exist for the reason that Gaussian noise signal is not absolutely integrable. Nevertheless, in the signal processing of FMCW radar, Gaussian noise is sampled in limited time period and the amplitude of each sample is limited by the ADC. In this condition, the discrete Fourier transform (DFT) of the finite-length sampled Gaussian noise exists:

$$\begin{aligned} Z(k) &= \sum_{m=0}^{M-1} z(m)e^{-j2\pi km/M} \\ &= \sum_{m=0}^{M-1} z(m)\cos\left(\frac{2\pi}{M}km\right) \\ &\quad + j\cdot\left[-\sum_{m=0}^{M-1} z(m)\sin\left(\frac{2\pi}{M}km\right)\right] \\ &= Z_{\mathrm{R}}(k) + j\cdot Z_{\mathrm{I}}(k), \quad 0 \le k \le \frac{M}{2}-1, \end{aligned} \quad (2)$$

where $z(m)$, $0 \le m \le M-1$, denotes the finite-length sampled sequence of Gaussian noise. The values that $z(m)$ can take on follow the Gaussian distribution $N(0,\sigma^2)$. Furthermore, the values at any pair of time indexes of $z(m)$ are statistically independent and identically distributed. Since $z(m)$ is a real sequence, $Z(k)$ is conjugate-symmetric about the index $M/2$ and only $M/2$ points of $Z(k)$ need to be calculated.

According to Equation (2), each element of the sequence $Z_{\mathrm{R}}(k)$ or $Z_{\mathrm{I}}(k)$ can be seen as a linear combination of Gaussian random variables. Therefore, the values that $Z_{\mathrm{R}}(k)$ or $Z_{\mathrm{I}}(k)$ can take on also follow Gaussian distribution. The mean of the values that $Z_{\mathrm{R}}(k)$ can take on is

$$\mathrm{E}[Z_{\mathrm{R}}(k)] = \sum_{m=0}^{M-1}\mathrm{E}[z(m)]\cos\left(\frac{2\pi}{M}km\right) = 0. \quad (3)$$

The variance can be expressed as

$$\begin{aligned} \mathrm{D}[Z_{\mathrm{R}}(k)] &= \mathrm{E}\left[Z_{\mathrm{R}}{}^2(k)\right] - \left[\mathrm{E}\left[Z_{\mathrm{R}}(k)\right]\right]^2 \\ &= \sum_{m=0}^{M-1}\sum_{n=0}^{M-1}\mathrm{E}[z(m)z(n)]\cos\left(\frac{2\pi}{M}km\right)\cos\left(\frac{2\pi}{M}kn\right). \end{aligned} \quad (4)$$

The elements of the sequence $z(m)$ are independent real variables ($\mathrm{E}[z(m)\,z(n)] = 0$ for $m \ne n$), thus we have

$$\begin{aligned} \mathrm{D}[Z_{\mathrm{R}}(k)] &= \sum_{m=0}^{M-1}\mathrm{E}\left[z^2(m)\right]\cos^2\left(\frac{2\pi}{M}km\right) \\ &= \frac{M}{2}\sigma^2 + \frac{\sigma^2}{4}\sum_{m=0}^{M-1}\left(e^{j\frac{2\pi}{M}2km} + e^{-j\frac{2\pi}{M}2km}\right). \end{aligned} \quad (5)$$

From the above, we get

$$\mathrm{D}\left[Z_{\mathrm{R}}(k)\right] = \begin{cases} M\sigma^2, & k = 0, \\ \dfrac{M}{2}\sigma^2, & 1 \le k \le \dfrac{M}{2}-1. \end{cases} \quad (6)$$

In the same manner, we can derive the mean and the variance of the values that $Z_{\mathrm{I}}(k)$ can take on. Finally, we obtain

$$\begin{cases} Z_{\mathrm{R}}(k) \sim N\left(0, \dfrac{M}{2}\sigma^2\right), & 1 \le k \le \dfrac{M}{2}-1, \\ Z_{\mathrm{I}}(k) \sim N\left(0, \dfrac{M}{2}\sigma^2\right), & 1 \le k \le \dfrac{M}{2}-1, \end{cases} \quad (7)$$

where the values of $Z_{\mathrm{R}}(0)$ and $Z_{\mathrm{I}}(0)$ are not considered for the reason that the DC component of beat signal is not useful for target detection.

Furthermore, it can be demonstrated that:

$$\begin{cases} \mathrm{Cov}[Z_{\mathrm{R}}(k_1)Z_{\mathrm{R}}(k_2)] = 0, \quad 1 \le k_1, k_2 \le \dfrac{M}{2}-1, k_1 \ne k_2, \\ \mathrm{Cov}[Z_{\mathrm{I}}(k_1)Z_{\mathrm{I}}(k_2)] = 0, \quad 1 \le k_1, k_2 \le \dfrac{M}{2}-1, k_1 \ne k_2, \\ \mathrm{Cov}[Z_{\mathrm{R}}(k_1)Z_{\mathrm{I}}(k_1)] = 0, \quad 1 \le k_1 \le \dfrac{M}{2}-1. \end{cases} \quad (8)$$

For $0 \le k \le M/2-1$, $Z_{\mathrm{R}}(k)$ or $Z_{\mathrm{I}}(k)$ is a stationary Gaussian noise sequence, and $Z_{\mathrm{R}}(k)$ and $Z_{\mathrm{I}}(k)$ are independent with each other at the same index. Therefore, each variable of $|Z(k)|$ has a Rayleigh distribution [6] and the PDF of them is

$$p_{\mathrm{fa}}(x) = \frac{x}{{\sigma_f}^2}\exp\left(-\frac{x^2}{2{\sigma_f}^2}\right), \quad (9)$$

where ${\sigma_f}^2 = M\sigma^2/2$.

The false alarm probability of FMCW radar, denoted as P_{fa}, is the probability that the spectral magnitudes of Gaussian noise will exceed the threshold A_{T}:

$$P_{\mathrm{fa}} = \int_{A_{\mathrm{T}}}^{\infty} p_{\mathrm{fa}}(x)dx = \exp\left(-\frac{{A_{\mathrm{T}}}^2}{2{\sigma_f}^2}\right). \quad (10)$$

3.2 Detection Probability

According to Equation (1), the sampled sequence of the beat signal $s(t)$ is

$$s(m) = A\cos\left[2\pi\Delta F_{\mathrm{m}}\tau\frac{m}{M} + 2\pi f_0\tau\right]. \tag{11}$$

The DFT of $s(m)$ can be expressed as:

$$\begin{aligned} S(k) &= \sum_{m=0}^{M-1} s(m)e^{-j2\pi km/M} \\ &\approx \frac{M}{2}A\cdot\mathrm{sinc}(\pi\delta)\cos(\phi) \\ &\quad + j\cdot\frac{M}{2}A\cdot\mathrm{sinc}(\pi\delta)\sin(\phi) \\ &\approx S_{\mathrm{R}}(k) + j\cdot S_{\mathrm{I}}(k) \qquad k = 0,1,...,\frac{M}{2}-1, \end{aligned} \tag{12}$$

Where $\phi = 2\pi f_0\tau - (M-1)(k-\Delta F_m\tau)\pi/M$ and $\delta = k - \Delta F_m\tau$.

Assuming $v(m)$ is the sampled sequence of the beat signal along with Gaussian noise, the DFT of $v(m)$ can be expressed as:

$$\begin{aligned} V(k) &= \sum_{m=0}^{M-1}\left[s(m)+z(m)\right]e^{-j2\pi km/M} \\ &= S_{\mathrm{R}}(k) + Z_{\mathrm{R}}(k) + j\cdot\left[S_{\mathrm{I}}(k) + Z_{\mathrm{I}}(k)\right] \\ &= V_{\mathrm{R}}(k) + j\cdot V_{\mathrm{I}}(k) \qquad k = 0,1,...,\frac{M}{2}-1. \end{aligned} \tag{13}$$

On the basis of Section 3.1, we can obtain

$$\begin{cases} V_{\mathrm{R}}(k) \sim N\left(A_f\cdot\cos(\phi), {\sigma_f}^2\right), 1 \le k \le \frac{M}{2}-1, \\ V_{\mathrm{I}}(k) \sim N\left(A_f\cdot\sin(\phi), {\sigma_f}^2\right), 1 \le k \le \frac{M}{2}-1. \end{cases} \tag{14}$$

Where $A_f = MA\cdot\mathrm{sinc}(\pi\delta)/2$.

For $0 \le k \le M/2\text{-}1$, it can be demonstrated that $V_{\mathrm{R}}(k)$ and $V_{\mathrm{I}}(k)$ are independent with each other at the same index. Therefore, each element of $|V(k)|$ has a Rice distribution [6] and the probability density function is

$$p_{\mathrm{d}}(x) = \frac{x}{{\sigma_f}^2}\exp\left(-\frac{x^2+{A_f}^2}{2{\sigma_f}^2}\right)\mathrm{I}_0\left(\frac{xA_f}{{\sigma_f}^2}\right), \tag{15}$$

Where $\mathrm{I}_0(Z)$ is the modified Bessel function of zero order and argument Z.

The detection probability of FMCW radar, denoted as P_{d}, is the probability that the spectral magnitudes of beat signal embedded in Gaussian noise will exceed the threshold A_{T}:

$$P_{\mathrm{d}} = \int_{A_{\mathrm{T}}}^{\infty} p_{\mathrm{d}}(x)dx. \tag{16}$$

For convenience, we use S_f/N_f to represent ${A_f}^2/{\sigma_f}^2$. It should be noted that S_f/N_f is not the signal-to-noise ratio of the beat signal, which is at the input of the spectrum analyser. The relation between S_f/N_f and the signal-to-noise ratio S/N of the beat signal is

$$\frac{S_f}{N_f} = \frac{M\cdot\mathrm{sinc}^2(\pi\delta)}{2}\frac{A^2}{2\sigma^2} = \frac{M\cdot\mathrm{sinc}^2(\pi\delta)}{2}\cdot\frac{S}{N}. \tag{17}$$

3.3 Detection Loss Caused by Picket Fence Effect

From Section 3.1 and 3.2, we can see that the mathematical expressions for the false alarm probability and detection probability of FMCW radar have the same forms as those of pulse radar. The discrete magnitude spectrum of beat signal is an exact analogue of the sampled video signal of pulse radar.

In pulse radar, the maximum sampled amplitude is lower than the maximum pulse amplitude owing to the offset between the sampling time instants and the position of the pulse. The resulting loss is called as "sampling loss" [4]. In FMCW radar, a point target corresponds to a Sinc-shape pulse in the beat signal spectrum. The spectrum is discretized due to the picket fence effect. The offset between the frequency-domain sampling instants and the position of the Sinc-shape pulse peak can cause a loss in S_f/N_f, which can be expressed as:

$$\begin{aligned} (L_f)_{\mathrm{dB}} &= \left(\frac{S_f}{N_f}\right)_{\max,\mathrm{dB}} - \left(\frac{S_f}{N_f}\right)_{\mathrm{dB}} \\ &= \left(\frac{M}{2}\cdot\frac{S}{N}\right)_{\mathrm{dB}} - \left(\frac{M\cdot\mathrm{sinc}^2(\pi\delta)}{2}\cdot\frac{S}{N}\right)_{\mathrm{dB}} \\ &= 10\log\left[1/\mathrm{sinc}^2(\pi\delta)\right], \ -0.5 \le \delta \le +0.5. \end{aligned} \tag{18}$$

In light of the "sampling loss" in pulse radar, we can call this kind of loss as "frequency-domain sampling loss". It can be observed from Equation (15) and (16) that the frequency-domain sampling loss can degrade the detection probability.

4 Proposed Threshold Detection Method

By adopting zero-padding FFT, the frequency-domain sampling interval can be narrowed, and the corresponding frequency-domain sampling loss can be expressed as

$$(L_f)_{\mathrm{dB}} = 10\log\left[1/\mathrm{sinc}^2(\pi\delta_{\mathrm{P}})\right]. \tag{19}$$

Where $\delta_P = k/P - \Delta F_m\tau$ and $-1/2P \le \delta_P \le +1/2P$. It is obviously that the frequency-domain sampling loss will approach to 0dB when P is large enough. However, the computation time of zero-padding FFT will become extremely long when the number of points is very large.

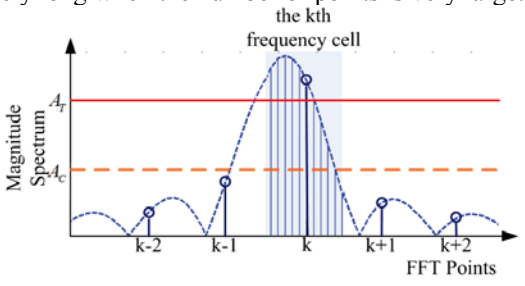

Figure 2. Local magnitude spectrum corresponding to one target.

In practice, there is no need to zoom the whole spectrum when the targets number is low. We can pick out the possible frequency cells (*A*s shown in Figure 2, the frequency range, which is centred at a FFT sample and has the same length with the FFT bin, is considered as a frequency cell.)

containing targets, and then use the local spectrum zooming method to alleviate the frequency-domain sampling loss. In Chirp z transform (CZT), the starting frequency point and frequency-domain sampling interval can be chosen arbitrarily [7]. CZT has been applied as a local spectrum zooming method for the improvement of ranging accuracy of FMCW radar [8].

In this paper, we propose a threshold detection method that combines FFT and CZT. As indicated in Figure 3, the M-point FFT is implemented firstly and the magnitude of each FFT point, which is expressed as $|V(k)|$, is compared with A_C ($A_C < A_T/\mathrm{sinc}(\pi/2)$). If $|V(k)|$ is less than A_C, we consider that there is no target in the kth frequency cell and no further processing is needed. If $|V(k)|$ exceeds A_C, CZT will be performed in the kth frequency cell. The final threshold detection with the threshold level A_T is performed on the spectral magnitudes of CZT.

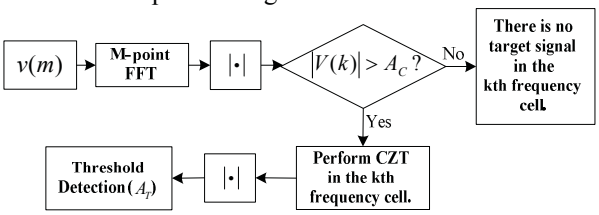

Figure 3. Flow diagram of our proposed threshold detection method.

A_C can be regarded as a low threshold. Utilizing the low threshold, we can exclude most useless frequency cells and save a large amount of computation time. The value of A_C should be small enough to deal with the worst situation when the pulse peak locates at the midpoint of a FFT bin. However, too much useless frequency cells will be included if A_C is too small. Therefore, the value of A_C should be chosen with thorough consideration.

5 Simulation Results

Simulation was carried out in Matlab R2014a to verify the effectiveness of the proposed threshold detection method. In the simulation, the SNR of the beat signal was calculated according to the well known radar equation [3]:

$$R^4 = \frac{P_t G_t G_r \sigma \lambda^2}{(4\pi)^3 k T_0 B F_n L_s (S/N)}, \qquad (20)$$

where P_t is the transmitter power, G_t is the transmitting antenna gain, G_r is the receiving antenna gain, σ is the RCS of the target, λ is the wavelength of the transmitted signal, k is the Boltzmann's constant, T_0 is the standard temperature, F_n is the receiver noise figure, L_s is the system loss, B is the half-power bandwidth of the band-pass filter, S/N is the signal-to-noise ratio of the beat signal. Parameters of a 77GHz automotive radar were utilized (Table 1) and the target was assumed as a nonfluctuating model with $\sigma = 20\mathrm{m}^2$.

In our proposed detection method, the value of the threshold A_T was calculated according to Equation (16), assuming false alarm probability is 10^{-8}. In addition, a moderate value of A_T /1.8 was chosen for A_C and the number of CZT points in one frequency cell was set to 512.

Table 1. Parameters of a 77GHz automotive radar.

Parameter	Value	Parameter	Value
f_0 (GHz)	76.5	G_r (dB)	20
ΔF_m (MHz)	300	F_n (dB)	13
T (ms)	1	L_s (dB)	4
P_t (dBm)	10	B (KHz)	500
G_t (dB)	20	FFT points M	1024

First of all, the detection probabilities of our proposed method and FFT based detection method were tested. The relationship between detection probability and detection range are shown in Figure 4. When using the FFT-based detection method, which simply performs threshold detection on the M-point FFT magnitudes, detection probability fluctuates widely with detection range owing to the large frequency-domain sampling loss near the midpoints of FFT bins (dash line). In contrast, the detection probability is much more stable and maintains a much higher level when using our proposed method (solid line). But since A_C is not small enough, the loss at the midpoint is still larger than anywhere else in a FFT bin. The false alarm probability was also tested by simulation. Because the proposed method takes advantage of the correlation property of the samples in the main lobe of the Sinc pulse, the false alarm probability is smaller than 10^{-8}, which is assumed before the simulation. The test result shows that the false alarm probability of our proposed method is 1.3729×10^{-9}.

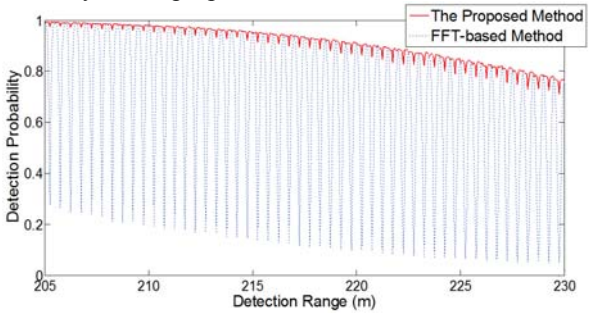

Figure 4. Detection probability of the proposed detection method and FFT-based threshold detection method.

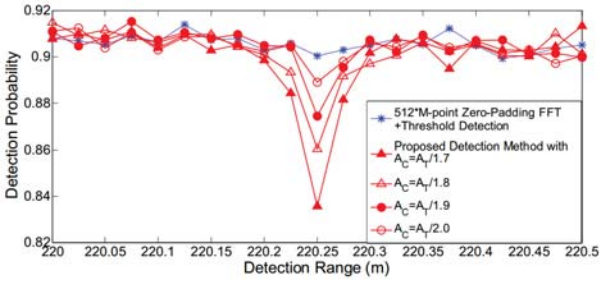

Figure 5. Detection probability of the proposed detection method with different values of A_C (within the FFT bin around the range of 220.25 m).

A_C is a key parameter in the proposed method. We can observe in Figure 5 that the detection probability at the midpoint of the FFT bin increases as A_C becomes smaller. When A_C equals $A_T/2$, the detection probability of the pro-

posed method is very close to that of the 512×M-point zero-padding FFT. However, the operation time increases with the decline of A_C. Figure 6 shows the operation time of the proposed detection method with different values of A_C. In the test, all the values of parameters in CZT were calculated in advance, and the convolution sum was implemented using FFT-based method. We can also observe in Figure 6 that the high speed advantage of the proposed method will disappear when the number of targets becomes large.

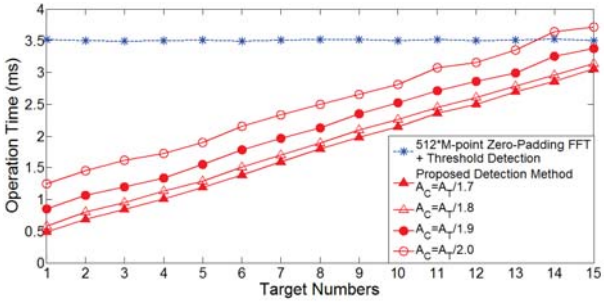

Figure 6. Operation time versus target numbers for the proposed detection method with different values of A_C (tested in Matlab R2014a).

6 Conclusions

The mathematical expressions for false alarm probability and detection probability of FMCW radar were derived in this paper. Frequency-domain sampling loss was introduced to describe the degradation of the detection performance caused by the picket fence effect of FFT. The novel threshold detection method proposed in this paper can effectively alleviate the frequency-domain sampling loss while reducing the false alarm probability. Compared with the detection method based on zero-padding FFT, the method proposed here has similar detection performance but faster operational speed when the number of targets is low. The proposed method is most suitable for single target applications such as microwave level measurement.

Acknowledgments

This paper was supported by National Nature Science Foundation of China (No. 61301213), Research Funds for Ministerial Key Laboratory of JMT, Nanjing University of Science and Technology(No. 3092013012200Y), Jiangsu research innovation project of graduate student (No. KYLX_0364).

References

[1] Stove, A.G., “Linear FMCW radar techniques”, IEE proceedings-F, 1992, 139, (5), pp. 343–350.

[2] Grzywacz, A., “Experimental investigations of digital signal processing techniques in an FMCW radar for naval application”. Proc. 14th Int. Conf. Microwaves Radar and Wireless Communications, 2002, 3, pp. 757–763.

[3] Skolnik, M.I., “Introduction to radar systems” (McGraw-Hill, 2001, 3rd edn.).

[4] D'Aloisi, D., Di Vito, A., Galati, G., “Sampling losses in radar signal detection”, Journal of the Institution of Electronic and Radio Engineers, 1986, 56, (6), pp. 237–242.

[5] Wu, Y., Linnartz, J.P.M.G., “Detection performance improvement of FMCW Radar using frequency shift”. Proceedings of the 32nd WIC Symposium on Information Theory in the Benelux, Brussels, Belgium, May 2011, pp. 1-8.

[6] Proakis, J.G., Salehi, M., “Digital Communications” (McGraw-Hill, 2008, 5th edn.).

[7] Mitra, S.K., “Digital Signal Processing：A Computer-Based Approach” (McGraw-Hill, 2001, 3rd edn.).

[8] Liu, B., Liu, J., “A method of the realization of high accuracy in FMCW ranging system”, Journal of Electronic Measurement and Instrument, 2001, 15, (3), pp. 41-45.